



Original article

Potent direct inhibitors of factor Xa based on the tetrahydroisoquinoline scaffold

Rami A. Al-Horani, Akul Y. Mehta, Umesh R. Desai*

Department of Medicinal Chemistry and Institute for Structural Biology and Drug Discovery, Virginia Commonwealth University, Richmond, VA 23298, United States

ARTICLE INFO

Article history:

Received 14 March 2012

Received in revised form

12 June 2012

Accepted 15 June 2012

Available online 23 June 2012

Keywords:

Anticoagulant

Direct inhibition

Structure–activity relationships

Coagulation enzymes

Tetrahydroisoquinoline synthesis

ABSTRACT

Direct inhibition of coagulation factor Xa (FXa) carries significant promise for developing effective and safe anticoagulants. Although a large number of FXa inhibitors have been studied, each can be classified as either possessing a highly flexible or a rigid core scaffold. We reasoned that an intermediate level of flexibility will provide high selectivity for FXa considering that its active site is less constrained in comparison to thrombin and more constrained as compared to trypsin. We studied several core scaffolds including 1,2,3,4-tetrahydroisoquinoline-3-carboxylic acid for direct FXa inhibition. Using a genetic algorithm-based docking and scoring approach, a promising candidate **23** was identified, synthesized, and found to inhibit FXa with a K_i of 28 μM . Optimization of derivative **23** resulted in the design of a potent dicarboxamide **47**, which displayed a K_i of 135 nM. Dicarboxamide **47** displayed at least 1852-fold selectivity for FXa inhibition over other coagulation enzymes and doubled PT and aPTT of human plasma at 17.1 μM and 20.2 μM , respectively, which are comparable to those of clinically relevant agents. Dicarboxamide **47** is expected to serve as an excellent lead for further anticoagulant discovery.

© 2012 Elsevier Masson SAS. All rights reserved.

1. Introduction

Anticoagulants represent the basis for treatment and prevention of thromboembolic disorders [1]. *A priori*, the inhibition of any coagulation enzyme can be expected to reduce or prevent clotting, yet most strategies have targeted two serine proteases, factor IIa (FIIa, or thrombin) and factor Xa (FXa), which belong to the common pathway of the coagulation cascade [2]. Of these, thrombin plays a major role in a number of physiologically relevant responses that rely on its catalytic activity [3,4]. Thus, inhibition of thrombin not only reduces cleavage of fibrinogen to fibrin, a key aspect of clotting, but also other processes such as platelet activation, platelet aggregation and angiogenesis. On the other hand, FXa has a rather limited role in comparison, which is to generate thrombin.

Several lines of evidence suggest that FXa may represent a better target for anticoagulation. FXa's contribution to amplification of the coagulation signal is higher than that of thrombin [5,6]. Its

occurrence earlier in the coagulation pathway suggests that a FXa inhibitor may be more effective in blocking progression of a coagulation signal than a thrombin inhibitor [7,8]. Recent results with indirect parenteral and direct oral FXa inhibitors have shown reduced bleeding complications [9]. Also, thrombin inhibitors have been associated with rebound hypercoagulability [10,11], while peptidomimetic inhibitors have been shown to inhibit both free as well as clot-bound FXa [12,13].

FXa can be inhibited through two major pathways including an indirect, antithrombin-dependent pathway [14,15] or a direct FXa targeting pathway [16–18]. Designing indirect FXa inhibitors that activate antithrombin is challenging and has been achieved primarily with heparin-based molecules [14,19], although efforts are afoot to design effective non-saccharide-based antithrombin activators [15,20,21]. In contrast, designing direct inhibitors of FXa has been much more productive and has led to several clinically relevant peptidomimetics, e.g., rivaroxaban [22], apixaban [23], DPC423 [24], and others, that target FXa's active site.

A large number of scaffolds have been studied for direct inhibition of FXa including the aminopiperidines [25], piperazines [26], diaminocycloalkanes [27], lactams [28,29], oxazolidinones [30], amino acids (e.g., glycine, proline, and β -aminopropionate) [31,32], anthranilamides [33], isoxazoles [34], pyrazoles [24,35], indazoles [36], indoles [37,38], and dihydropyrazolopyridinones [23,39]. The overall philosophy in the design of these scaffolds is to have a three-component system, which includes a core scaffold and two hydrophobic arms that provide a non-linear geometry considered

Abbreviations: ABH3CA, 2-azabicyclo[2.2.1]heptane-3-carboxylic acid; APTT, activated partial thromboplastin time; FIIa, factor IIa (thrombin); FXa, factor Xa; HS, hill slope; P2CA, piperidine-2-carboxylic acid; P3CA, piperidine-3-carboxylic acid; PA, phenylalanine; PT, prothrombin time; THIQ, 1,2,3,4-tetrahydroisoquinoline; THIQ3CA, 1,2,3,4-tetrahydroisoquinoline-3-carboxylic acid; THP2CA, 1,2,3,6-tetrahydropyridine-2-carboxylic acid.

* Corresponding author. Department of Medicinal Chemistry, Virginia Commonwealth University, 800 East Leigh Street, Suite 212, PO Box 980133, Richmond, VA 23219, United States. Tel.: +1 804 828 7328; fax: +1 804 827 3664.

E-mail address: urdesai@vcu.edu (U.R. Desai).

important for FXa recognition. In addition, a key design principle has also been flexibility of the core scaffold. The core scaffolds studied to date can be classified into either a highly flexible class or a fairly rigid class.

It is known that trypsin's active site is much open than FXa's, which in turn possesses an active site that is more open than that of thrombin. This allows trypsin to work upon practically any arginine containing sequence, while thrombin prefers a fairly rigid proline containing sequence. Thus, we hypothesized that an intermediate level of flexibility in the core scaffold will engineer high selectivity for FXa inhibition.

In this work, we studied several core scaffolds with variable flexibility to design potent direct FXa inhibitors. Of the scaffolds studied, the 1,2,3,4-tetrahydroisoquinoline-3-carboxylic acid (THIQ3CA) scaffold possessing an intermediate level of flexibility was found to be the best. Molecular modeling-based identification of an initial hit **23** was transformed into the discovery of a potent direct FXa inhibitor **47** with a K_i of 135 nM. This molecule selectively targeted FXa in comparison to the enzymes of the coagulation and digestive systems, and doubled clotting times at 17–20 μ M, which are comparable to those of the inhibitors being studied in clinical trials [40]. The work with a library of 39 molecules has revealed interesting structure–activity relationships (SAR) that identify optimal structural units for engineering good FXa inhibition properties. The lead THIQ3CA dicarboxamide **47** is expected to serve as an excellent starting point for further advanced design.

2. Results and discussion

2.1. Designing the tetrahydroisoquinoline-3-carboxylic acid scaffold as a potential factor Xa inhibitor scaffold

The glycine and β -aminopropionate-based inhibitors are examples of a highly flexible core scaffold, while aromatic scaffolds, e.g., aminobenzoic acids, pyrazoles, and indazoles, are examples of fairly rigid scaffolds. An intermediate level of flexibility in the core scaffold has not been studied to date for direct FXa inhibition. A large number of scaffolds possess intermediate level of flexibility including tetrahydroisoquinoline (THIQ), tetrahydroquinoline, tetrahydroquinazoline, dihydrocoumarin, and dihydroindole. In each of these, the five- or six-membered rings are flexible, yet full flexibility is restricted due to ring fusion. Of these, we focused on the THIQ scaffold, which is a widely explored privileged structure [15,41–44]. To enable a non-linear structure for FXa recognition, we introduced a carboxylic acid group at the 3-position of the THIQ scaffold to arrive at THIQ3CA scaffold.

The designed THIQ3CA scaffold was first investigated *in silico* to assess its potential in binding in factor Xa active site as well as to identify a potential inhibitor for synthesis. A library of THIQ3CA structures was prepared by introducing substituents at positions 2 and 3. A large group of aromatic and non-aromatic carboxylic acid and amine arms at positions 2 and 3 were studied to identify potential 'hits' (see [Supplementary Information](#)). The virtual library of resulting THIQ3CA dicarboxamides was then computationally docked into active site of human FXa and scored using genetic algorithm-based screening technique developed in our laboratory earlier [15]. As positive controls, two well-established direct FXa inhibitors, apixaban and rivaroxaban, were also studied in an identical manner.

The GOLD-based docking and scoring strategy identified several hits, of which THIQ3CA dicarboxamide **23**, containing a 5-chlorothiophen-2-yl moiety (also present in rivaroxaban), was identified as a promising candidate. Fig. 1A shows a comparison of the predicted bound form of **23** with apixaban. Both molecules adopted a rather similar binding mode in which the 5-chlorothiophenyl-carbonyl group was found to be oriented toward

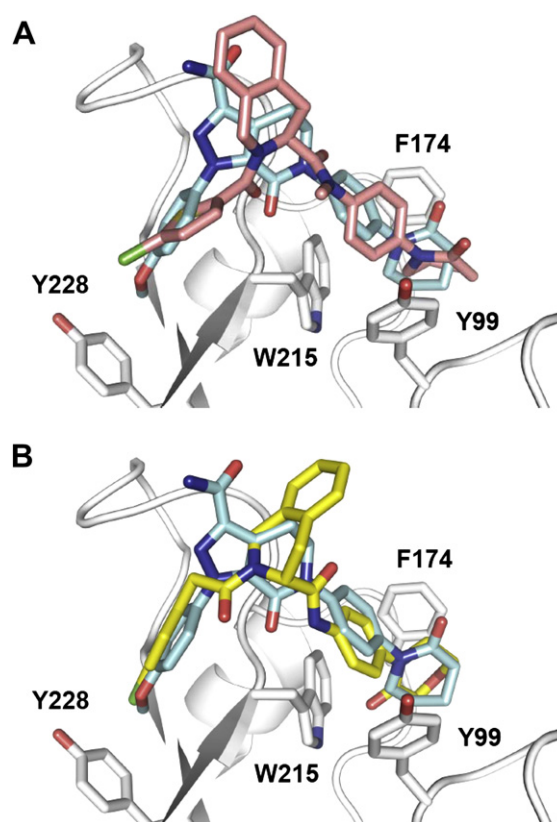
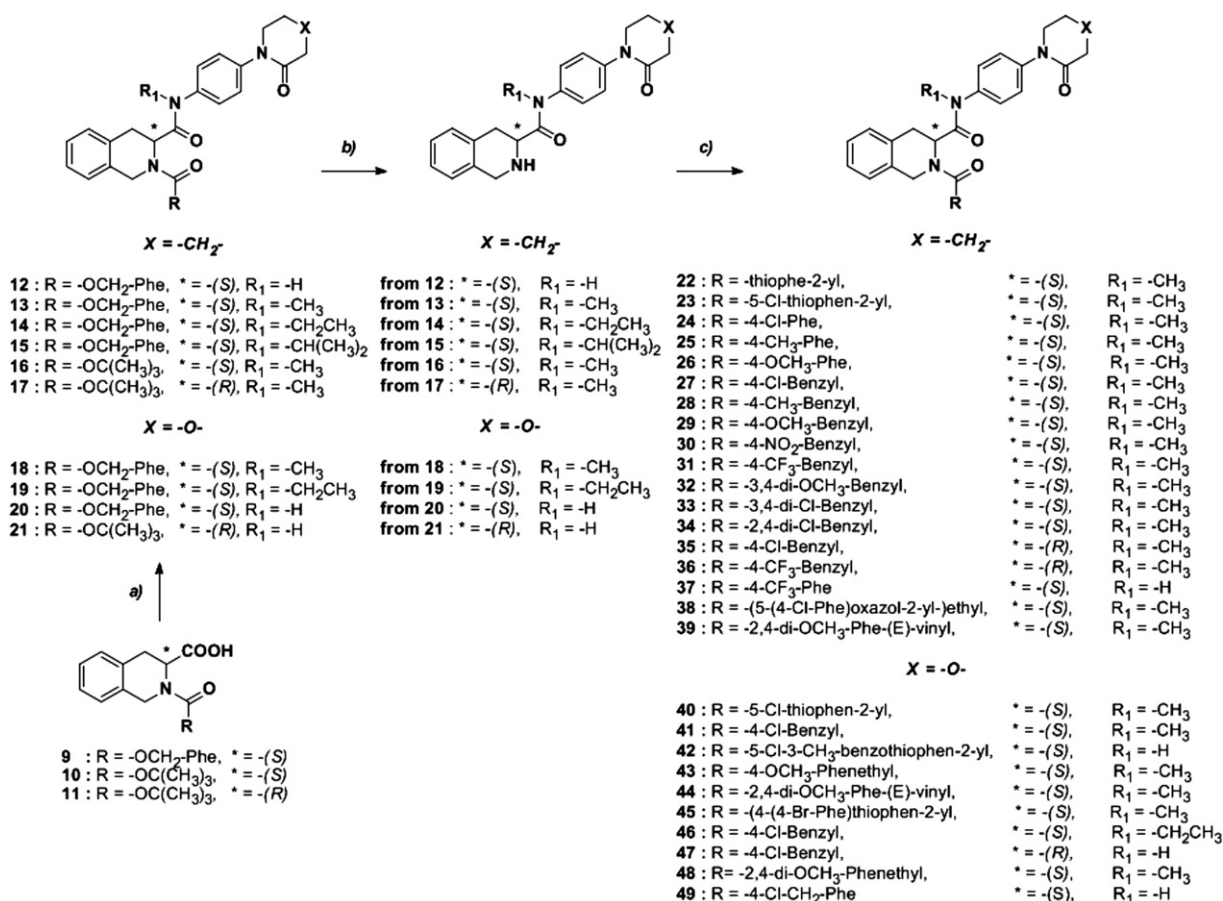


Fig. 1. Virtual screening of a library of potential THIQ3CA-based inhibitors docked and scored onto the active site of FXa (PDB: 2P16) using GOLD resulted in the design of **23** (A: GOLD score of 69.3, Carbons in pink) that appeared to mimic the binding of well known potent FXa inhibitors. The virtual library of THIQ3CA-based dicarboxamides contained structural modifications in arms A_N and A_C . Apixaban (GOLD score of 93.7, Carbons in blue) and rivaroxaban (GOLD score of 87.2, structure not shown) were also docked and scored as positive controls. Systematic structural modifications led to the design of the most potent THIQ3CA dicarboxamide **47** (B: GOLD score of 77.2, Carbons in yellow). See text for details.

the S1 subsite and the 4-(piperidin-2-one)- N^1 -methylaniline moiety oriented into the S4 subsite. Comparison of the binding geometry with rivaroxaban suggested similar corresponding features (not shown). THIQ3CA dicarboxamide **23** was synthesized in three high yielding steps and evaluated for its direct human FXa inhibition potential (see below). An IC_{50} of 55.9 μ M, corresponding to a K_i of 28 μ M, was measured validating the potential of the THIQ3CA core scaffold in direct human FXa inhibition investigation.

2.2. Synthesis of THIQ3CA-based potential FXa inhibitors

Based on the structure of **23**, a library of THIQ3CA dicarboxamides was designed. The synthesis of the targeted THIQ3CA analogs was achieved using a facile three-step strategy of amidation, deprotection, and amidation that relied on the availability of the two arms, A_N and A_C , at positions 2 and 3, respectively [45]. Each A_N structure designed as a part of the library was commercially available and was introduced using standard amidation reaction (see [Scheme 1](#)). In contrast, arm A_C at position 3 of THIQ3CA required pre-assembly. This arm was synthesized by aromatic nucleophilic substitution in which 4-bromoaniline derivatives **4a–4c** were reacted with either valerolactam **5a** or morpholin-3-one **5b** to quantitatively give the corresponding 4-substituted aniline derivatives **8a–8g** [46]. Likewise, substituted anilines **8h–8j** containing the piperazine side chain were also



Scheme 1. a) Appropriate amine (**8a–8g**), HOBT·H₂O, DMAP, EDCI, CH₂Cl₂, rt/overnight, 73–89%, b) For Cbz-protected intermediates: 10% Pd(OH)₂, (1:1) CH₃OH: *t*-butanol, H₂, rt/overnight, 65–72%. For Boc-protected intermediates: (1:1) TFA:CH₂Cl₂, rt/4 h, 75%, c) Appropriate organic acid, EDCI, DMAP, CH₂Cl₂, rt/overnight, 70–95%.

included in the study (see [Supplementary Information Scheme S1](#) for synthetic and characterization details).

To introduce either arm A_N or A_C through an amidation reaction, the THIQ3CA core was first appropriately protected, which involved either esterification of the 3-carboxylic acid or *t*-butoxycarbonylation (Boc group) or carbonylbenzyloxycarbonylation (Cbz group) of the ring nitrogen. For example, THIQ3CAs **9–11** were amidated using amines **8a–8g** to yield Boc- or Cbz-protected THIQ3CA monocarboxamides **12–21** in 73–89% yield ([Scheme 1](#)). The Boc or Cbz protecting group of **12–21** was then removed using either mild acid [47] or catalytic hydrogenation [48], respectively, to afford the corresponding free form in 65–75% yield. The free form of **12–21** was then amidated at the 2 position with twenty one carboxylic acids in the presence of EDCI to yield the targeted THIQ3CA dicarboxamides **22–49** in 70–95% yield ([Scheme 1](#)). This strategy was also exploited for the synthesis of THIQ3CA dicarboxamides **50–55**, **59**, and **62** that contain additional variations on arms A_N and A_C (see [Supplementary Information Scheme S2 and S3](#)).

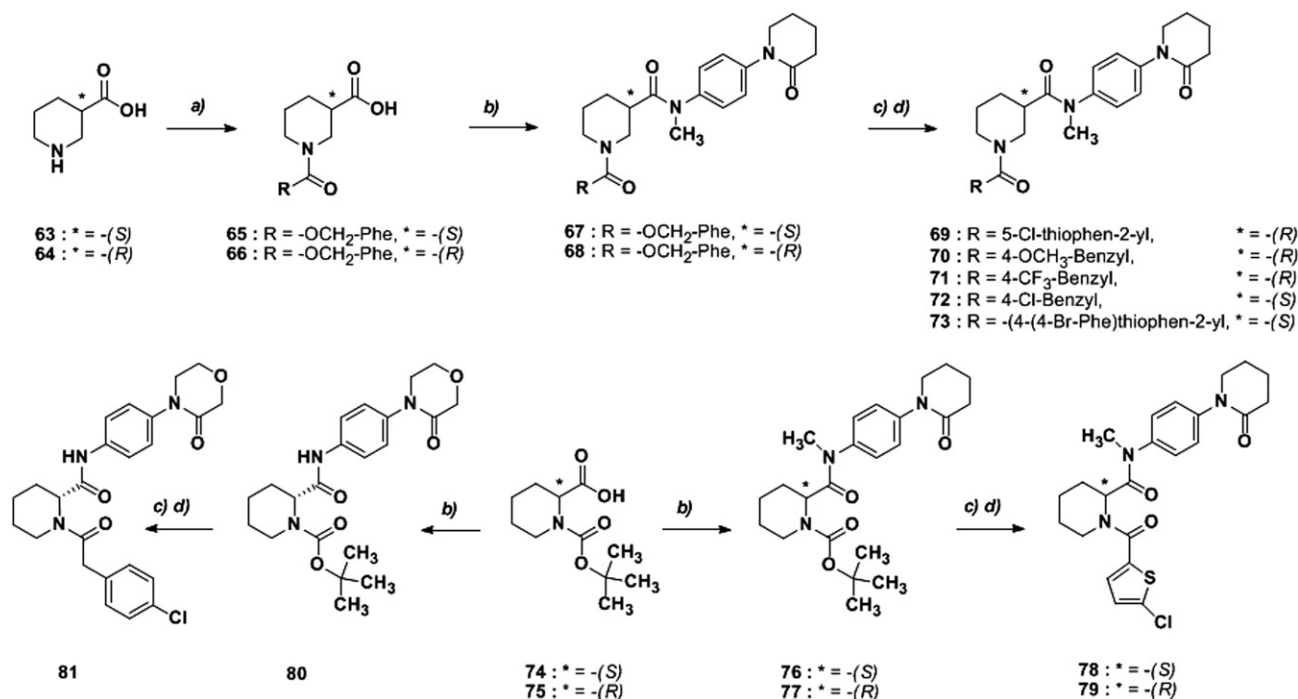
To assess the effect of flexibility for FXa inhibition, we targeted three core scaffolds that afford greater flexibility than the THIQ3CA scaffold as well as can help assess the importance of configurational geometry. These scaffolds were: 1) a ring opened variant of THIQ3CA core, the phenylalanine (PA) derivative **62**; 2) mono-cyclic dicarboxamides **69–73** belonging to the piperidine-3-carboxylic acid (P3CA) class; and 3) mono-cyclic dicarboxamides **78**, **79** and **81** belonging to the piperidine-2-carboxylic acid (P2CA) class ([Scheme 2](#)). These molecules were synthesized in a manner similar to the THIQ3CA scaffold using the amidation, deprotection, and amidation strategy.

To understand the importance of the aromatic ring of the THIQ3CA scaffold, and yet mimic its flexibility, we targeted 1) a partially unsaturated, cyclic ring system, i.e., (S)-1,2,3,6-tetrahydropyridine-2-carboxylic acid (THP2CA) and 2) a bridged system, i.e., (1*R*,3*S*,4*R*)-2-azabicyclo[2.2.1]heptane-3-carboxylic acid (ABH3CA) ([Scheme 3](#)). The synthesis of either scaffold started with the Boc-protected carboxylic acid **82** or **85**, which was converted in three steps to dicarboxamide **84** or **87**, respectively, in excellent yield.

Overall, we synthesized twenty eight THIQ3CA, one PA, five P3CA, three P2CA, one THP2CA and one ABH3CA dicarboxamides using a simple three-step protocol. The molecules were purified using standard flash chromatography system and were characterized using ¹H and ¹³C NMR spectroscopy and ESI-MS (see [Supplementary Information](#)).

2.3. Inhibition potential of the library of FXa inhibitors

Direct inhibition of FXa was measured by a chromogenic substrate hydrolysis assay in 20 mM TrisHCl buffer, pH 7.4, at 37 °C, as reported earlier [49]. In this assay, hydrolysis of the substrate by FXa results in a linear increase in absorbance at 405 nm, the slope of which corresponds to residual enzyme activity. The change in residual enzyme activity as a function of the concentration of the potential inhibitor is plotted on a logarithmic scale and fitted by the logistic dose–response relationship 2 to derive the potency (IC₅₀), efficacy (ΔY = Y_M – Y₀) and Hill Slope (HS) of inhibition [18,49]. [Fig. 2](#) shows representative inhibition profiles for **20**, **47**, **49**, and **51**, which are THIQ3CA derivatives, and **62** and **81**, which are PA and

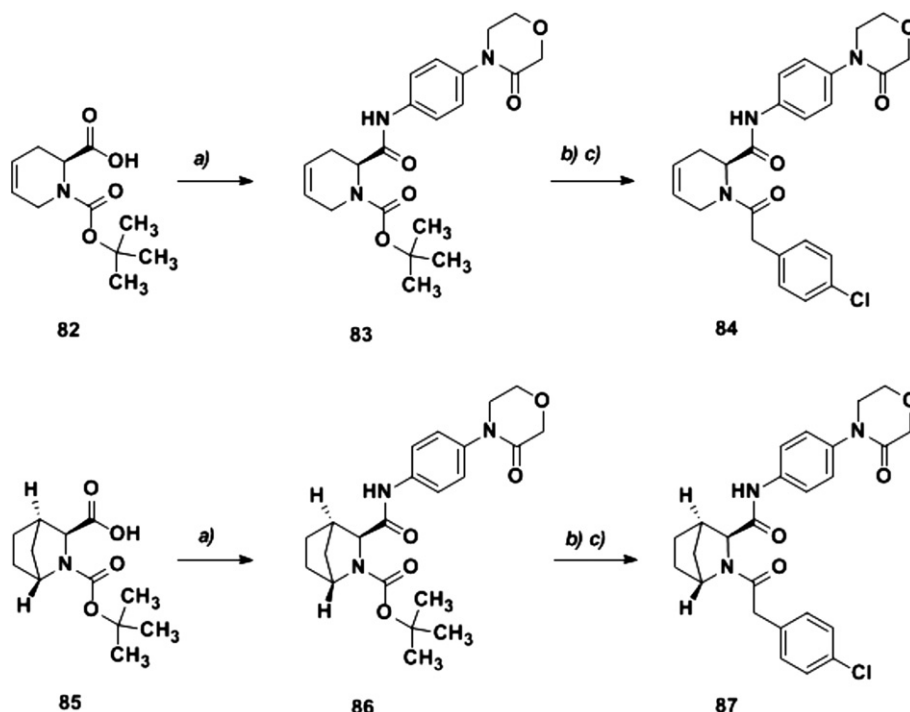


Scheme 2. a) Benzyl chloroformate, Et₃N, THF, rt/5 h, 70–73%, b) **8b** or **8c**, HOBT·H₂O, DMAP, EDCI, CH₂Cl₂, rt/overnight, 73–89%, c) For Cbz-protected intermediates: 10% Pd(OH)₂, (1:1) CH₃OH: *t*-butanol, H₂, rt/overnight, 65–72%. For Boc-protected intermediates: (1:1) TFA:CH₂Cl₂, rt/4 h, 75%, d) Appropriate organic acid, EDCI, DMAP, CH₂Cl₂, rt/overnight, 70–95%.

P2CA derivatives, respectively. Similar profiles were measured for other THIQ3CA, P2CA, P3CA, THP2CA, and ABH3CA derivatives, except for the variation in potency of inhibition. The *HS* of inhibition was found to be in the range of 0.7–1.2, which suggests absence of the complications arising from non-specific binding or aggregation. The *IC*₅₀ values of the FXa inhibitors studied in this work were found to exhibit a wide range of activity (high μ M to nM), which provide valuable structure–activity relationships.

2.4. Structural optimization of arm A_C of the THIQ3CA scaffold

Our early molecular modeling studies suggested that arm A_C at the 3-position of the THIQ3CA core structure bound in the S4 subsite of the FXa active site. An intermediate **13**, synthesized early in the library and containing *N*-(*N*-methylanilin-4-yl)piperidin-2-one as the A_C arm, had shown a reasonable *IC*₅₀ of 16.4 μ M. This formed the starting point for studying the S4 subsite substitutions



Scheme 3. a) **8b**, HOBT·H₂O, DMAP, EDCI, CH₂Cl₂, rt/overnight, b) (1:1) TFA:CH₂Cl₂, rt/4 h, c) 4-Chlorophenyl acetic acid, EDCI, DMAP, CH₂Cl₂, rt/overnight, 70–95%.

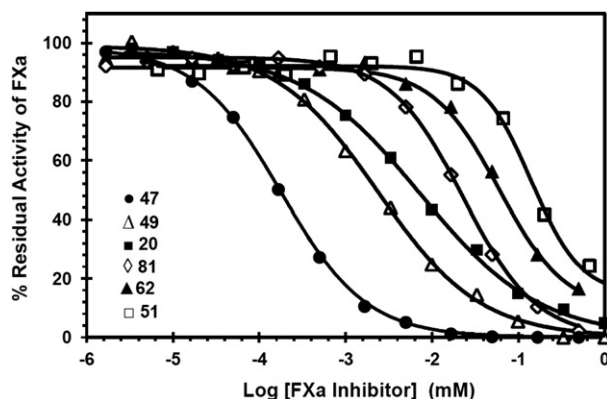


Fig. 2. Direct inhibition of FXa by designed THIQ3CA and related dicarboxamides. The inhibition of human FXa was determined spectrophotometrically through the chromogenic substrate hydrolysis assay at pH 7.4 and 37 °C. Solid lines represent sigmoidal fits to the data to obtain IC_{50} , Y_M , Y_0 , and HS , as described in the [Experimental methods](#) section. Experiments were performed in duplicate or triplicate ($SE < 20\%$). See text for details.

(Table 1). To optimize the structure of the A_C arm, two levels of structural modifications were introduced. These included 1) variation in the carboxamide N -substituent and 2) variation in the *para*-substituent of the aniline moiety. Replacing the N -methyl group of **13** with ethyl (inhibitor **14**) and isopropyl (inhibitor **15**) groups resulted in no significant change, however, N -demethylation as in **12** reduced the IC_{50} by 1.7-fold suggesting the possibility of the formation of a hydrogen bond. This was however not substantiated by molecular modeling (not shown) and we speculated that the alkyl group on the nitrogen may be inducing a conformational preference that is not favorable for binding in the S_4 subsite.

To optimize the *para*-substituent of the aniline moiety, we relied on the extensive literature that abounds in such optimizations [2,16,50]. The moieties preferred at this position include the piperidone, morpholinone, piperidine, piperazine and other rings. Yet, introducing piperidine and piperazine moieties at the *para* position of the aniline was catastrophic. The piperidine-containing derivative **53** and the piperazine-containing derivatives **54** and **55** displayed an un-quantifiable IC_{50} of $>500 \mu M$ (Table 1). Molecular modeling suggested that the *para* substituent helps orient the adjacent aromatic ring for better interaction with Tyr99, Phe174, and Trp215 of the S_4 subsite (not shown), in a manner similar to that observed with rivaroxaban and apixaban [23,30]. Thus, we studied the morpholin-3-one moiety (derivative **20**, Table 1), which exhibited a much improved IC_{50} of $6.0 \mu M$. The results indicated a significant contribution of the carbonyl group of morpholin-3-one for the THIQ3CA inhibitors.

2.5. Structural optimization of arm A_N of the THIQ3CA scaffold

Molecular modeling suggested that the A_N arm at position 2 of the THIQ3CA core fits into S_1 subsite of the FXa active site. The initial hit **13** ($IC_{50} = 16.4 \mu M$) containing the Cbz group as the A_N arm was used as the starting point for studying the S_1 subsite substitutions. Considering that the A_N arm of **13** is structurally less defined than its A_C arm, we decided to explore a wider range of moieties to replace the Cbz group. Thus, optimal chain length of A_N , the nature of its aromatic ring, and the position and number of substituents on the aromatic ring were studied.

Replacing the A_N arm of **13** with thiophenyl carbonyl (**22**), 5-chlorothiophenyl carbonyl (**23**), *p*-chlorophenyl carbonyl (**24**), *p*-methylphenyl carbonyl (**25**) or *p*-methoxyphenyl carbonyl (**26**) arm resulted in 1.2–12.7-fold reduction in potency (Table 2). Extending the length of the linker by one carbon atom resulted in

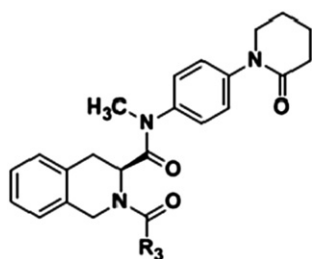
Table 1
Optimization of the A_C arm (position 3) of THIQ3CA scaffold for FXa inhibition

Inhibitor	R_1	R_2	IC_{50} (μM)
12	–H		9.9 ± 0.2
13	–CH ₃		16.4 ± 0.4
14	–CH ₂ CH ₃		20 ± 1
15	–CH(CH ₃) ₂		19 ± 2
18	–CH ₃		12.8 ± 0.2
19	–CH ₂ CH ₃		19 ± 6
20	–H		6.0 ± 0.8
50	–H	–Cl	>500
53	–H		>500
54	–H		>500
55	–H		>500

significant improvement in IC_{50} . Dicarboxamide **27** containing a 4-chlorophenyl acetyl side chain exhibited an IC_{50} of $1.3 \mu M$, which was the first high affinity inhibitor ($K_i = 0.65 \mu M$) designed in the THIQ3CA series. Yet, most subsequent modifications failed to enhance potency further. For example, one or more electron

Table 2

Optimization of the A_N arm (position 2) of THIQ3CA scaffold containing the piperidone moiety in the A_C arm for FXa inhibition



Inhibitor	R ₃	IC ₅₀ (μM)
16		221 ± 19
22		42 ± 2
23		56 ± 2
24		197 ± 39
25		209 ± 31
26		19 ± 2
27		1.3 ± 0.1
28		14 ± 3
29		34 ± 1
30		85 ± 19
31		335 ± 50
32		246 ± 58
33		18 ± 2
34		1.3 ± 0.2
38		103 ± 8

donating (–CH₃, –OCH₃) as well as one or more electron withdrawing (–Cl, –CF₃, –NO₂) substituents on the phenylacetyl side chain weakened the potency by 1–262-fold (Table 2).

Considering the observations made with the A_C structural variants, we studied the morpholin-3-one containing THIQ3CA derivatives also for optimization of the A_N arm. Table 3 shows the results obtained in the morpholin-3-one series. Replacing the Cbz group of parent **18** (IC₅₀ = 12.8 μM) with thiophenyl carbonyl (**40**), *p*-methoxyphenyl propanoyl (**43**), or 2,4-dimethoxyphenyl propanoyl (**48**) resulted in considerable loss of activity. Yet, as in the piperidone series described above, introducing a 4-chlorophenyl acetyl side chain for the Cbz group resulted in an IC₅₀ of 1.1 μM.

Analysis of the above results indicated that the best inhibitors carried a 7-atom arm A_N (at position 2), e.g., **13**, **26**, **27**, **28**, and **41**. Within this category, a 7-atom arm containing a small, lipophilic electron-withdrawing group (–Cl) is optimal. This group appears to be the *p*-chlorophenylacetyl moiety, as exemplified by a considerable increase in affinity observed with **27**, **34** and **41**, and a loss in affinity for derivative **49** (Tables 2 and 3). Thus, FXa appears to preferentially recognize the chlorophenyl moiety in the THIQ3CA series of inhibitors.

2.6. Rational design of analog **47**

The majority of inhibitors described above possessed (*S*)-chirality at position 3. To assess whether an (*R*)-isomer would be

Table 3

Optimization of the A_N arm (position 2) of THIQ3CA scaffold containing the morpholinone moiety in the A_C arm for FXa inhibition

Inhibitor	R ₁	R ₃	IC ₅₀ (μM)
40	–CH ₃		36 ± 3
41	–CH ₃		1.1 ± 0.1
42	–H		5.4 ± 0.9
43	–CH ₃		190 ± 16
45	–CH ₃		>500
48	–CH ₃		>500
49	–H		2.9 ± 0.4

better, we studied THIQ3CA derivative **35**, which is a stereoisomer of **27** ($IC_{50} = 1.3 \mu\text{M}$). This stereochemical inversion resulted in a 1.5-fold increase in the activity (Table 4). This led to a hypothesis that introducing optimal features derived on arms A_N and A_C into a single THIQ3CA derivative may lead to the most potent FXa inhibitor designed so far. Thus, analog **47** was designed, which contained a morpholin-3-one moiety, a *p*-chlorophenylacetyl unit, (*R*)-chirality at the 3-position, and *NH*-containing carboxamide at the 3-position. THIQ3CA derivative **47** displayed an IC_{50} of 270 nM ($K_i = 135 \text{ nM}$) and represents the highest potency observed in the THIQ3CA series.

The design of **47** reflects a truly additive phenomenon. Inhibitor **47** exhibits ~60-fold decrease in IC_{50} relative to the starting inhibitor **13** ($IC_{50} = 16.4 \mu\text{M}$), which can be rationalized from the 1.5-fold (morpholin-3-one) \times 2-fold (unsubstituted carboxamide) \times 1.5-fold (stereochemical inversion) \times 13-fold (4-chlorophenylacetyl moiety) increases found independently earlier. This is an interesting observation and appears to have considerable consistency across the series of molecules studied here.

2.7. THIQ3CA core is the most optimal scaffold

Based on the number of flexible carbons constituting the core scaffold, we reasoned that the open-chain PA core will be more flexible than the six-membered cyclic P2CA and P3CA cores, which in turn will exhibit greater flexibility than the unsaturated or bridged THP2CA and ABH3CA cores. The THIQ3CA core was likely to be similar to the unsaturated or bridged cores in terms of conformational flexibility. Table 5 displays the potency of selected PA,

P2CA, P3CA, THP2CA, ABH3CA, and THIQ3CA inhibitors. Overall, the potency of PA, P2CA, and P3CA dicarboxamide inhibitors was found to be weak (23–371 μM), while that for THP2CA, ABH3CA and THIQ3CA inhibitors were higher (0.27–56 μM). Comparison of the unsaturated or bridged six-membered scaffold with the THIQ3CA scaffold shows that the latter is the most optimal structure. For example, THP2CA derivative **84** and ABH3CA derivative **87** exhibit IC_{50} s of 9.1 and 10 μM , which are 33–37-fold greater than the 0.27 μM IC_{50} of the corresponding THIQ3CA derivative **47** (Table 5).

Within these broad results, we noticed interesting structure–activity dependence across the different core scaffolds studied here. Nearly all 5-chloro-thiophenyl containing derivatives, e.g., **23** and **40**, display weak inhibition potency in comparison to most *p*-chlorophenyl containing derivatives, e.g., **27** and **41** (Tables 2 and 3). This was against our expectation based on the well established high affinity of rivaroxaban, which contains the 5-chloro-thiophenyl side chain [22,30]. Another interesting observation was that morpholin-3-one ring consistently induces higher potency than the piperid-2-one ring. For example, morpholin-3-one-containing THIQ3CA derivatives **18**, **20**, and **40** have better activity than the corresponding piperid-2-one-containing derivatives **13**, **12**, and **23**, respectively (see Tables 1–3).

The above results suggest that the THIQ3CA core scaffold was the most optimal for FXa inhibition following optimization of its two arms A_N and A_C . Yet, the THP2CA and ABH3CA scaffolds are interesting. These are scaffolds are new, readily synthesizable and are relatively unexplored. Screening of a wider chemical space would help better understand their true potential for FXa inhibition.

2.8. Dicarboxamide **47** selectively inhibits factor Xa in comparison to other proteases of the coagulation and digestive systems

A critical goal of the molecular modeling-based rational design of THIQ3CA inhibitors was selectivity for targeting factor Xa. This enzyme is a trypsin-like serine protease with considerable homology with enzymes of the coagulation and digestive systems including FIIa, FVIIa, FIXa, FXIa, FXIIa, trypsin and chymotrypsin. Chromogenic substrate hydrolysis assays for each of these enzymes were performed in a manner similar to that for FXa. The assays were conducted at 37 °C using literature reported buffer systems that are as close to physiological conditions as possible (see Experimental methods for details). Initial screening was performed at a high, fixed concentration of the inhibitor (100–1000 μM) and fractional residual enzyme activity was measured from the initial rate of hydrolysis in the presence of the inhibitor to that in its absence.

The THIQ3CA inhibitors showed high selectivity for FXa inhibition. No coagulation enzyme was found to be inhibited by THIQ3CA inhibitors at concentrations less than 100 μM . With regard to digestive enzymes, moderate inhibition of chymotrypsin ($IC_{50} = 5–100 \mu\text{M}$) was noted with 4-chlorophenyl side chain containing inhibitors. The most potent FXa inhibitor **47** demonstrated a selectivity of at least 1852-fold over FIIa, FVIIa, FIXa, FXIa, and FXIIa (Table 6). Against trypsin and chymotrypsin, the selectivity of **47** was found to be at least 370- and 279-fold, respectively. Few rationally designed inhibitors have been able to achieve such high selectivity for factor Xa against other homologous enzymes [51,52].

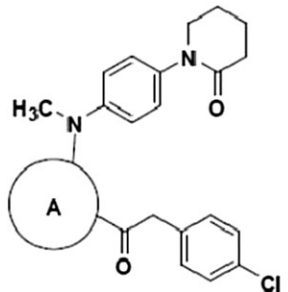
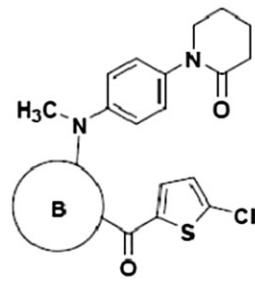
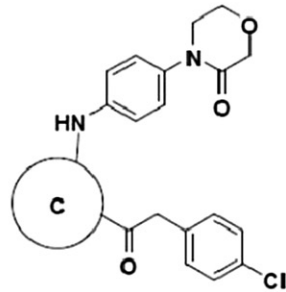
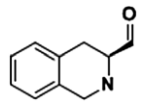
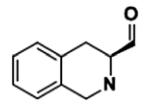
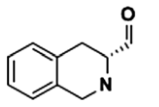
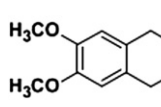
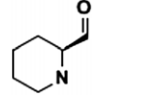
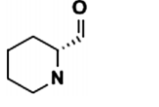
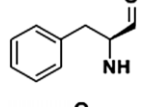
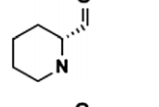
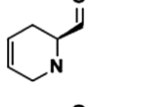
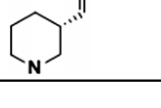
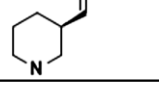
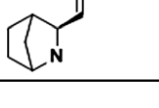
2.9. Prolongation of plasma clotting times by THIQ3CA, THP2CA and ABH3CA inhibitors

Clotting assays, prothrombin and activated partial thromboplastin time (PT and aPTT, respectively), are routinely used to assess anticoagulation potential of new enzyme inhibitors in an *in vitro* setting [18,53,54]. Whereas PT measures the effect of an inhibitor on the extrinsic pathway of coagulation, aPTT measures the effect on

Table 4
Simultaneous optimization of both A_N A_C arms of THIQ3CA scaffold for optimal FXa inhibition

Inhibitor	R_1	X	Y	R_3	Chirality (*)	IC_{50} (μM)
35	–CH ₃	–CH ₂ –	–C(O)–		(<i>R</i>)-	0.9 \pm 0.1
36	–CH ₃	–CH ₂ –	–C(O)–		(<i>R</i>)-	311 \pm 56
37	–H	–CH ₂ –	–C(O)–		(<i>S</i>)-	13.3 \pm 1.4
46	–CH ₂ CH ₃	–O–	–C(O)–		(<i>S</i>)-	1.6 \pm 0.2
47	–H	–O–	–C(O)–		(<i>R</i>)-	0.27 \pm 0.03
52	–CH ₃	–CH ₂ –	–SO ₂ –		(<i>S</i>)-	151 \pm 36

Table 5
Comparison of the FXa inhibition potential of different scaffolds

								
Inhibitor	A	IC ₅₀ (μM)	Inhibitor	B	IC ₅₀ (μM)	Inhibitor	C	IC ₅₀ (μM)
27		1.3 ± 0.1	23		56 ± 2	47		0.27 ± 0.03
59		7.8 ± 0.4	78		358 ± 16	81		23 ± 2
62		54 ± 5	79		99 ± 7	84		9 ± 2
72		371 ± 59	69		69 ± 7	87		10 ± 3

the intrinsic pathway. The prolongation of the human plasma clotting time as a function of the concentration of the inhibitors followed a pattern typical of other well-studied anticoagulants (data not shown), except for the range of active concentrations. Table 7 lists the concentrations of selected potent FXa inhibitors required to double the PT and aPTT. Overall, for the inhibitors studied, doubling the PT required 17–2347 μM concentration, while doubling of aPTT required 20–810 μM suggesting that most inhibitors essentially affect both pathways equally (Fig. 3). This is to be expected because of their selectivity for targeting FXa, which is an enzyme of the common pathway. The inhibitors studied included THIQ3CA derivatives **20**, **27**, **34**, **42**, **47**, and **49**, and THP2CA/ABH3CA derivatives **84** and **87**. Inhibitor **47** doubled the PT clotting time at 17.1 μM, which is comparable to razaxaban (3.8 μM) and DPC423 (4.9 μM), two direct FXa inhibitors being pursued in clinical trials [51].

3. Significance

Our work investigates the dependence of direct FXa inhibition on the flexibility of core scaffold and attempts to optimize the

structure of two arms A_N and A_C of a bifunctional cyclic ring system. We discovered interesting structural preference for both arms and a fine additive relationship that culminated in the design of THIQ3CA analog **47**, which displays direct inhibition IC₅₀ of 270 nM (K_i = 135 nM). Synthetically, the FXa inhibitors were readily assembled using three high yielding steps, which required room temperature conditions and avoided harsh reactions. Our work suggests that the morpholin-3-one ring engineers better inhibitor potential than any other ring system; that the nitrogen of the carboxamide group at position-3 should be optimally unsubstituted; that a (*R*)-stereochemistry at position-3 is more preferred than its (*S*)-enantiomer; and that a 7-atom A_N arm containing a *para*-chloro substituted aromatic ring is critical for potent, direct FXa inhibition. It is also worth mentioning that the A_N and A_C arms should be adjacent to each other (1,2-substitution) rather than one carbon away (1,3-disubstitution). These conclusions may help design more potent molecules.

Table 6
Selectivity of inhibition by THIQ3CA dicarboxamide **47**.

Protease	IC ₅₀ (μM)	Selectivity index
Human FIIa	>500	>1852
Human FVIIa	>1000	>3703
Human FIXa	>1000	>3703
Human FXIa	>500	>1852
Human FXIIa	>500	>1852
Bovine trypsin	>100	>370
Bovine chymotrypsin	75.3 ± 13.4	279

Table 7
Effect of designed FXa dicarboxamide inhibitors on human plasma clotting time.

Inhibitor	PT (μM)	aPTT (μM)
20	1387	ND ^a
27	71	80
34	219	260
42	2160	ND ^a
47	17.1	20.2
49	645	614
84	952	810
87	2347	ND ^a

^a Not determined.

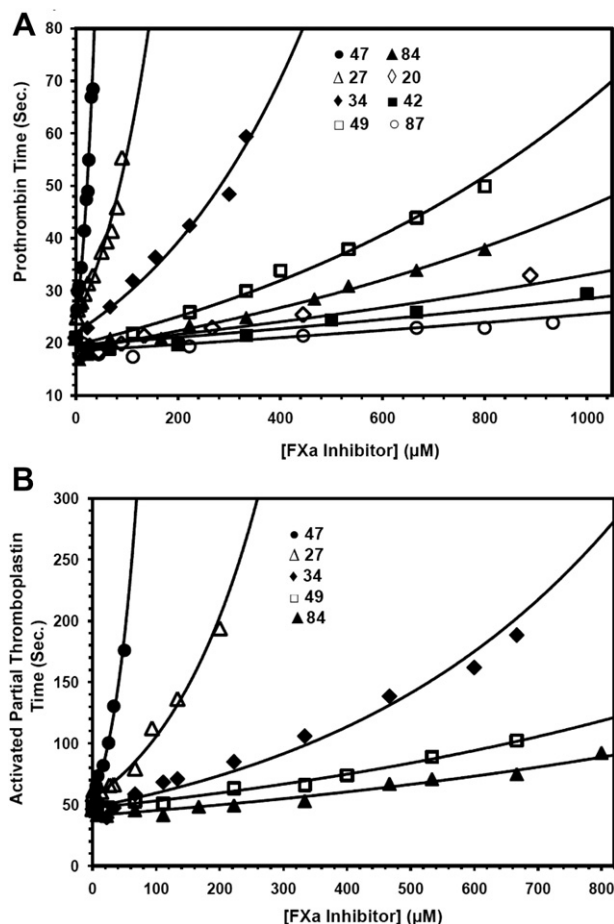


Fig. 3. Prolongation of clotting time as a function of concentration of designed THIQ3CA and related dicarboxamides in either prothrombin time assay (PT) (A) or activated partial thromboplastin time assay (aPTT) (B). Solid lines are trend lines from which the concentration necessary to double clotting time was deduced. Clotting assays were performed in duplicate ($SE \leq 10\%$) as described in [Experimental methods](#).

4. Experimental methods

4.1. Chemicals, reagents, and analytical chemistry

Anhydrous CH_2Cl_2 , THF, CH_3CN , DMF, toluene, and acetone were purchased from Sigma–Aldrich (Milwaukee, WI) or Fisher (Pittsburgh, PA) and used as such. Other solvents used were of reagent gradient and used as purchased. Analytical TLC was performed using UNIPLATE™ silica gel GHLF 250 μm pre-coated plates (ANALTECH, Newark, DE). Column chromatography was performed using silica gel (200–400 mesh, 60 Å) from Sigma–Aldrich. Chemical reactions sensitive to air or moisture were carried out under nitrogen atmosphere in oven-dried glassware. Reagent solutions, unless otherwise noted, were handled under a nitrogen atmosphere using syringe techniques. Flash chromatography was performed using Teledyne ISCO (Lincoln, NE) Combiflash RF system and disposable normal silica cartridges of 30–50 μ particle size, 230–400 mesh size and 60 Å pore size. The flow rate of the mobile phase was in the range of 18–35 ml/min and mobile phase gradients of ethyl acetate/hexanes and CH_2Cl_2/CH_3OH were used to elute compounds.

4.2. Chemical characterization of compounds

1H and ^{13}C NMR were recorded on Bruker-400 MHz spectrometer in either $CDCl_3$, CD_3OD , or acetone- d_6 . Signals, in part per

million (ppm), are either relative to the internal standard (tetramethyl silane, TMS) or to the residual peak of the solvent. The NMR data are reported as chemical shift (ppm), multiplicity of signal (s = singlet, d = doublet, t = triplet, q = quartet, dd = doublet of doublet, m = multiplet), coupling constants (Hz), and integration. Compounds with dicarboxamide functionalities exhibit amide rotamerism resulting in complexity of NMR signals. ESI-MS of compounds were recorded using Waters Acquity TQD MS spectrometer in positive ion mode. Samples were dissolved in methanol and infused at a rate of 20 $\mu L/min$. Mass scans were obtained in the range of 200–700 amu with a scan time of 1 s and a scan rate of 500 amu/s. The capillary voltage was varied between 3 and 4 kV, while the cone voltage ranged from 38 to 103 V. Ionization conditions were optimized for each compound to maximize the ionization of the parent ion. Generally, the extractor voltage was set to 3 V, the Rf lens voltage was 0.1 V, the source block temperature was set to 150 $^{\circ}C$, and the desolvation temperature was about 250 $^{\circ}C$. The purity of each final compound was greater than 95% as determined by uPLC-MS.

4.3. Proteins

Human plasma proteinases including FIIa, FXa, FXIa, FIXa, FVIIa, and recombinant tissue factor was obtained from Haematologic Technologies (Essex Junction, VT). FXIIa was purchased from Enzyme Research Laboratories (South Bend, IN). Bovine α -chymotrypsin and bovine trypsin were obtained from Sigma–Aldrich (St. Louis, MO). The substrates Spectrozyme TH, Spectrozyme FXa, Spectrozyme FXIIa, Spectrozyme FIXa, Spectrozyme VIIa, and Spectrozyme CTY were obtained from American Diagnostica (Greenwich, CT). Factor XIa substrate, S-2366, trypsin substrate, S-2222, were obtained from Diapharma (West Chester, OH). Factor Xa and FVIIa were prepared in 20 mM TrisHCl buffer, pH 7.4, containing 100 mM NaCl, 2.5 mM $CaCl_2$, 0.1% PEG8000, and 0.02% Tween80. FIXa was prepared in 20 mM TrisHCl buffer, pH 7.4, containing 100 mM NaCl, 2.5 mM $CaCl_2$, 0.1% PEG8000, 0.02% Tween80, and 33% v/v Ethyleneglycol. Other enzymes were prepared in 50 mM TrisHCl buffer, pH 7.4, containing 150 mM NaCl, 0.1% PEG8000, and 0.02% Tween80.

4.4. Modeling factor Xa and the virtual library of (S)-THIQ3CA dicarboxamides

Sybyl 8.1 (Tripos Associates, St. Louis, MO) was used for modeling of FXa-inhibitor complexes. The structure of human FXa (ID: 2P16) [23] was acquired from the Protein Data Bank (www.rcsb.org). To prepare the protein structure for modeling experiments, hydrogen atoms were added, while inorganic ions and water molecules were removed. Individual atoms were assigned Gasteiger–Hückel charges. Energy minimization was then performed using a Tripos force field so as to reach a terminating gradient of 0.5 kcal/mol Å² or a maximum of 100,000 iterations.

(S)-THIQ3CA was modified *in silico* at positions 2 and 3 with appropriate substituents to “synthesize” a virtual chemical library of nearly 150 dicarboxamide derivatives. The different combinations at 2- and 3-positions included substituted derivatives of aromatic carboxylic acids and aromatic amines, respectively. These acids and amines were further substituted at varying positions with halogen, *t*-butyl, cyclopropyl, methoxy, amino-methyl, substituted phenyl, substituted imidazole, pyridine, pyridine-2-one, *N*-oxide pyridine, *N*-methyl piperazine, or cyclic amides such as piperidone and morpholinone (See [Supplementary Information](#)). The resulting molecules were assigned Gasteiger–Hückel charges and were then energetically minimized using a Tripos force field until a terminating gradient of 0.5 kcal/mol Å² or a maximum of 100,000 iterations.

4.5. Docking and scoring

Docking of the (S)-THIQ3CA dicarboxamides onto the active site of FXa was performed with GOLD 5.1 (Cambridge Crystallographic Data Center, UK). The docking experiment was performed as reported earlier [15]. The binding site in human FXa was defined to include all atoms within 6 Å of the co-crystallized ligand. The docking protocol was validated by docking ligand for which the adopted docking pose was found to have RMSD < 1 Å relative to that reported in the crystal structure [23]. Docking was driven by the GOLD scoring function, while for ranking the docked solutions; a linear, modified form of the same scoring function Eq. (1) was used, as reported earlier [15]. In this equation, HB_{EXT} and VDW_{EXT} are the “external” (nonbonded interactions taking place between the ligand and the target protein) hydrogen bonding and van der Waals terms, respectively.

$$\text{GOLD}_{\text{Score}} = \text{HB}_{\text{EXT}} + 1.375 \times \text{VDW}_{\text{EXT}} \quad (1)$$

4.6. FXa inhibition studies

Direct inhibition of FXa was measured by a chromogenic substrate hydrolysis assay, as reported earlier [49] using a microplate reader (FlexStation III, Molecular Devices) at wavelength of 405 nm and incubating temperature of 37 °C. Generally, each well of the 96-well microplate had 185 µL pH 7.4 buffer to which 5 µL potential FXa inhibitor (or solvent reference) was added, to which 5 µL FXa (stock conc. 43.5 nM) was further added. After 10 min incubation at 37 °C, 5 µL FXa substrate (stock conc. 5 mM) was rapidly added and the residual FXa activity was measured from the initial rate of increase in absorbance at 405 nm. The concentration of the organic solvent in which the inhibitors were dissolved was maintained constant and was less than 2.5% (v/v). Stocks of FXa inhibitors were prepared at 20 mM concentration and then serially diluted to give twelve different aliquots spanning a range of 0.015–500 µM in the plate wells. Each inhibitor was studied in duplicate or triplicate at each concentration. Relative residual FXa activity at each concentration of the inhibitor was calculated from the ratio of FXa activity in the presence and absence of the inhibitor. Logistic Eq. (2) was used to fit the dose-dependence of residual proteinases activity to obtain the potency (IC_{50}) and efficacy (ΔY) of inhibition. In this equation, Y is the ratio of residual factor Xa activity in the presence of inhibitor to that in its absence (fractional residual activity), Y_M and Y_0 are the maximum and minimum possible values of the fractional residual proteinase activity, IC_{50} is the concentration of the inhibitor that results in 50% inhibition of enzyme activity, and HS is the Hill slope (which was between 0.7 and 1.2 in all measurements). Nonlinear curve fitting resulted in Y_M , Y_0 , IC_{50} and HS values. The reported IC_{50} is an average of the two or three measurements with standard error (SE) of <20%. The efficacy of inhibition ΔY was found to be >80% for each studied FXa inhibitor.

$$Y = Y_0 + \frac{Y_M - Y_0}{1 + 10^{(\log [I]_0 - \log IC_{50})/HS}} \quad (2)$$

4.7. Inhibition of proteases of the coagulation and digestive systems

The potential of the FXa inhibitors against coagulation enzymes including FIIa, FVIIa, FIXa, FXIa, and FXIIa, and digestive enzymes including trypsin and chymotrypsin was performed using chromogenic substrate hydrolysis assays reported in the literature [55]. These assays were performed using substrates appropriate for the enzyme being studied under conditions closest to the physiological condition (37 °C and pH 7.4), except for FIIa, which was performed

at 25 °C and pH 7.4. For selectivity analysis, a single concentration point assays was utilized in which 0.5–1 mM FXa inhibitor was tested in duplicate. The fractional residual enzyme activity was measured and if found to be less than 50%, the inhibition profile was measured over a range of inhibitor concentrations to determine the IC_{50} of the enzyme–inhibitor complex. The K_M of the substrate for its enzyme was used to identify the concentration of the substrate to be used for inhibition studies. The concentrations of enzymes and substrates in microplate cells were: 6 nM and 50 µM for FIIa; 0.765 nM and 345 µM for FXIa; 5 nM and 125 µM for FXIIa; 89 nM and 850 µM for FIXa; 8 nM and 1000 µM for FVIIa (along with 40 nM recombinant tissue factor); 72.5 ng/ml and 80 µM for bovine trypsin; and 500 ng/ml and 240 µM for bovine chymotrypsin.

4.8. Prothrombin time (PT) and activated partial thromboplastin time (aPTT)

Clotting time was measured in a standard one-stage recalcification assay with a BBL Fibrosystem fibrometer (Becton–Dickinson, Sparks, MD), as described previously [18]. For PT assays, thromboplastin was reconstituted according to the manufacturer's directions and warmed to 37 °C. A 10 µL sample of the FXa inhibitor, to give the desired concentration, was brought up to 100 µL with citrated human plasma, incubated for 30 s at 37 °C followed by addition of 200 µL of prewarmed thromboplastin. For the aPTT assay, 10 µL of inhibitor was mixed with 90 µL of citrated human plasma and 100 µL of prewarmed aPTT reagent (0.2% ellagic acid). After incubation for 4 min at 37 °C, clotting was initiated by adding 100 µL of prewarmed 25 mM $CaCl_2$ and time to clot noted. The data were fit to a quadratic trendline, which was used to determine the concentration of the inhibitor necessary to double the clotting time. Clotting time in the absence of an anticoagulant was determined in similar fashion using 10 µL of deionized water and/or appropriate organic vehicle and was found to be 21.0 s for PT and 46.4 s for aPTT.

4.9. General procedure for nucleophilic amidation of halogenated aniline derivatives **8a–8g**

An oven-dried, two-neck round bottom flask fitted with a condenser was charged with CuI (0.05 mmol) and K_2CO_3 (2.0 mmol) under nitrogen atmosphere. *N, N'*-dimethylethylenediamine (0.10 mmol), 4-haloaniline derivative (**4a–4c**) (1.0 mmol), piperidin-2-one (**5a**) or morpholin-3-one (**5b**) (1.5 mmol), and anhydrous toluene (1 mL) were added. The reaction mixture was stirred and refluxed overnight. The resulting mixture was allowed to reach RT and filtered through Celite, which was further washed with methanol (10 mL). The organic filtrate was concentrated *in vacuo* and the residue was purified by flash chromatography using gradient mobile phase of EtOAc/hexanes to afford the corresponding *para*-amidated aniline derivatives (**8a–8g**) as solid products in 65–90% yield. The full spectral characterization of these products is provided as [Supplementary Information](#).

4.9.1. 1-(4-Aminophenyl)piperidin-2-one (**8a**)

1H NMR ($CDCl_3$, 400 MHz): 7.00 (d, J = 8.76 Hz, 2 H), 6.56 (d, J = 8.76 Hz, 2 H), 3.56 (t, J = 5.44 Hz, 2 H), 2.52 (t, J = 5.24 Hz, 2 H), 1.92–1.89 (m, 4 H). ^{13}C NMR ($CDCl_3$, 100 MHz): 170.11, 146.25, 132.89, 127.19, 113.35, 52.17, 32.88, 23.04, 21.20. MS (ESI) calculated for $C_{11}H_{14}N_2O$, $[M + H]^+$, m/z 191.25, found for $[M + H]^+$, m/z 191.98.

4.10. General procedure for catalytic hydrogenation of nitro group for synthesis of **8i** and **8j**

4-Nitrophenylpiperazine (**7a** or **7b**) and 10% Pd/C was mixed in methanol (10 mL) containing concentrated HCl (2 mL). Hydrogen

gas was then pumped into the mixture at RT. After stirring the solution for 5 h, the catalyst was filtered on Celite and the organic filtrate concentrated *in vacuo* to afford the corresponding aniline derivative (**8h** and **8j**) in ~100% yield. The full spectral characterization of these products is provided as [Supplementary Information](#).

4.10.1. 1-(4-(4-Aminophenyl)piperazin-1-yl)ethanone (**8i**)

¹H NMR (CDCl₃, 400 MHz): 6.81 (d, *J* = 8.76 Hz, 2 H), 6.66 (d, *J* = 8.76 Hz, 2 H), 3.75 (t, *J* = 5.08 Hz, 2 H), 3.60 (t, *J* = 4.92 Hz, 2 H), 3.01 (t, *J* = 5.20 Hz, 2 H), 2.98 (t, *J* = 5.12 Hz, 2 H), 2.13 (s, 3 H). ¹³C NMR (CDCl₃, 100 MHz): 168.98, 144.04, 140.90, 119.32, 116.17, 51.55, 51.14, 46.51, 41.61, 21.33. MS (ESI) calculated for C₁₂H₁₇N₃O, [M + H]⁺, *m/z* 220.29, found for [M + H]⁺, *m/z* 220.15.

4.10.2. (4-(4-Aminophenyl)piperazin-1-yl)(thiophen-2-yl)methanone (**8j**)

¹H NMR (acetone-*d*₆, 400 MHz): 7.57 (d, *J* = 4.96 Hz, 1 H), 7.34 (d, *J* = 3.56 Hz, 1 H), 7.03 (d, *J* = 4.32 Hz, 1 H), 6.86 (d, *J* = 8.64 Hz, 2 H), 6.54 (d, *J* = 8.60 Hz, 2 H), 3.77 (t, *J* = 4.96 Hz, 4 H), 3.08 (t, *J* = 5.16 Hz, 4 H). ¹³C NMR (acetone-*d*₆, 100 MHz): 163.60, 148.27, 138.75, 129.72, 127.70, 122.94, 121.33, 120.06, 118.43, 116.14, 52.39, 51.20. MS (ESI) calculated for C₁₅H₁₇N₃OS, [M + H]⁺, *m/z* 288.39, found for [M + H]⁺, *m/z* 288.25.

4.11. General procedure for deprotection of *t*-butyloxycarbonyl (Boc) group of **16**, **17**, **21**, **61**, **76**, **77**, **80**, **83**, or **86**

To a solution of 1,2,3,4-tetrahydroisoquinoline carboxamides (**16**, **17**, **21**), phenylalanine carboxamide (**61**), piperidine-2-carboxamides (**76**, **77**, **80**), 1,2,3,6-tetrahydropyridine-2-carboxamides (**83**), or 2-azabicyclo[2.2.1] heptane-3-carboxamides (**86**) (1.0 mmol) in CH₂Cl₂ (5 mL), trifluoroacetic acid (TFA, 5 mL) was added drop-wise at 0 °C, and the mixture was warmed to RT. After stirring for 4 h, the reaction mixture was diluted with CH₂Cl₂ (25 mL) and neutralized by drop-wise addition of saturated aqueous NaHCO₃ (20 mL). The organic layer was separated and the aqueous phase was extracted with EtOAc (2 × 25 mL). The organic extracts were combined, washed with saturated NaCl solution (25 mL), and dried over anhydrous Na₂SO₄. Removal of the solvent under reduced pressure afforded the desired unprotected carboxamides in quantitative yields and sufficient purity (as indicated by TLC) to be directly used in the next reactions without any further treatment.

4.12. General procedure for deprotection of carbobenzyloxy (Cbz) group of **12–15**, **18–20**, **50**, **67** or **68**

1,2,3,4-tetrahydroisoquinoline carboxamides (**12–15**, **18**, **19**, **50**) or piperidine-3-carboxamides (**67** or **68**) and 10% Pd(OH)₂ on activated charcoal were mixed in CH₃OH: *tert*-butanol (1:1) mixture (10 mL). Hydrogen gas was then pumped into the mixture at RT. After stirring the solution overnight, the catalyst was filtered on Celite and the organic filtrate concentrated *in vacuo* to afford the corresponding desired unprotected carboxamides in quantitative yields and sufficient purity (as indicated by TLC) to be directly used in the next reactions without any further treatment.

4.13. General procedure for amine protection by carbobenzyloxy (Cbz) group in the synthesis of **65** or **66**

Piperidine-3-carboxylic acid (**63** or **64**) (1 mmol) was dissolved in dry THF (10 mL) and stirred at RT. Tri-ethylamine (Et₃N) (2 mmol) was then added followed by benzyl chloroformate (1.5 mmol). The reaction mixture became initially cloudy and turned to clear

solution after 5 h. The reaction mixture was then partitioned between acidified water (15 mL) and EtOAc (20 mL). The aqueous layer was further washed with EtOAc (2 × 20 mL). The organic extracts were combined, dried over anhydrous Na₂SO₃, filtered, and concentrated *in vacuo*. The *N*-Cbz protected product (**65** or **66**) was isolated as white solids by flash chromatography using gradient of EtOAc/hexanes as eluant in 70–73% yield.

4.13.1. (*S*)-1-(Benzyloxycarbonyl)piperidine-3-carboxylic acid (**65**)

¹H NMR (acetone-*d*₆, 400 MHz): 7.43–7.30 (m, 5 H), 5.15 (s, 2 H), 4.35–4.04 (m, 1 H), 3.93 (d, *J* = 12.08 Hz, 1 H), 3.18–3.02 (m, 1 H), 3.01–2.92 (m, 1 H), 2.53–2.46 (m, 1 H), 2.09–2.062 (m, 1 H), 1.75–1.66 (m, 2 H), 1.53–1.45 (m, 1 H). ¹³C NMR (acetone-*d*₆, 100 MHz): 174.88, 155.77, 138.25, 129.30, 128.70, 128.60, 67.49, 46.62, 44.90, 41.64, 27.87, 24.98. MS (ESI) calculated for C₁₄H₁₇NO₄, [M + H]⁺, *m/z* 264.30, found for [M + H]⁺, *m/z* 264.37.

4.13.2. (*R*)-1-(Benzyloxycarbonyl)piperidine-3-carboxylic acid (**66**)

¹H NMR (acetone-*d*₆, 400 MHz): 7.43–7.30 (m, 5 H), 5.15 (s, 2 H), 4.35–4.04 (m, 1 H), 3.93 (d, *J* = 12.08 Hz, 1 H), 3.18–3.02 (m, 1 H), 3.01–2.92 (m, 1 H), 2.53–2.46 (m, 1 H), 2.09–2.062 (m, 1 H), 1.75–1.66 (m, 2 H), 1.53–1.45 (m, 1 H). ¹³C NMR (acetone-*d*₆, 100 MHz): 174.88, 155.77, 138.25, 129.30, 128.70, 128.60, 67.49, 46.62, 44.90, 41.64, 27.87, 24.98. MS (ESI) calculated for C₁₄H₁₇NO₄, [M + H]⁺, *m/z* 264.30, found for [M + Na]⁺, *m/z* 286.28.

4.14. General procedure for amidation of 3-carboxylic acid to yield **12–21**, **50**, **53–55**, **59**, **61**, **67**, **68**, **76**, **77**, **80**, **83**, or **86**

To a stirred solution of the free carboxylic acid of (**9–11**, **58**, **60**, **65**, **66**, **74**, **75**, **82**, or **85**) (1.0 mmol) in anhydrous CH₂Cl₂ (5 mL) was added hydrated *N*-hydroxybenzotriazole (HOBT·H₂O, 1.1 mmol), DMAP (1.1 mmol), and 1-ethyl-3-(3-dimethylaminopropyl)carbodiimide (EDCI, 1.1 mmol) at RT under nitrogen atmosphere. Appropriate amine (**8a–8j** or 4-chloroaniline) (1.1 mmol) in anhydrous CH₂Cl₂ (5 mL) was then added dropwise. After stirring overnight, the reaction mixture was partitioned between 2.0 N HCl solution (20 mL) and CH₂Cl₂ (30 mL). The organic layer was washed further with 2 N HCl (2 × 10 mL) and saturated NaCl solution (20 mL), dried using anhydrous Na₂SO₄, and concentrated to give a crude, which purified by flash chromatography using gradient of CH₂Cl₂/CH₃OH as eluant to give the desired carboxamide product in 73–89% yield. The full spectral characterization of these products is provided as [Supplementary Information](#).

4.14.1. (*S*)-Benzyl 3-(4-(2-oxopiperidin-1-yl)phenylcarbamoyl)-3,4-dihydroisoquinoline-2(1H)-carboxylate (**12**)

¹H NMR (CDCl₃, 400 MHz): 7.50–7.27 (m, 6 H), 7.25–7.08 (m, 5 H), 7.06 (d, *J* = 8.44, 2 H), 5.23–5.12 (m, 2 H), 4.96–4.54 (m, 3 H), 3.55 (t, *J* = 5.00 Hz, 2 H), 3.40–3.30 (m, 1 H), 3.20–3.09 (m, 1 H), 2.52 (t, *J* = 5.00 Hz, 2 H), 2.00–1.87 (m, 4 H). ¹³C NMR (CDCl₃, 100 MHz): 170.23, 169.22, 156.94, 139.31, 136.09, 135.47, 134.33, 133.32, 128.64, 128.32, 128.07, 127.76, 127.23, 126.90, 126.58, 125.99, 120.87, 68.04, 64.35, 51.75, 45.08, 32.82, 30.31, 23.51, 21.41. MS (ESI) calculated for C₂₉H₂₉N₃O₄, [M + H]⁺, *m/z* 484.57, found for [M + Na]⁺, *m/z* 506.3.

4.14.2. (*S*)-Benzyl 3-(4-chlorophenylcarbamoyl)-3,4-dihydroisoquinoline-2(1H)-carboxylate (**50**)

¹H NMR (CDCl₃, 400 MHz): 7.50–7.35 (m, 3 H), 7.34–7.26 (m, 2 H), 7.25–7.18 (m, 4 H), 7.17–7.00 (m, 4 H), 5.39–5.10 (m, 2 H), 4.96–4.49 (m, 3 H), 3.35–3.21 (m, 1 H), 3.20–3.3.03 (m, 1 H). ¹³C NMR (CDCl₃, 100 MHz): 169.12, 157.30, 136.24, 135.95, 133.44, 132.70, 129.08, 128.81, 128.70, 128.57, 128.43, 128.11, 127.77, 126.78, 125.94, 121.13, 68.19, 57.04, 45.11, 28.30. MS (ESI) calculated for

$C_{24}H_{21}ClN_2O_3$, $[M + H]^+$, m/z 421.90, found for $[M + Na]^+$, m/z 443.26.

4.14.3. (S)-tert-Butyl 6-(4-(3-oxomorpholino)phenylcarbamoyl)-5,6-dihydropyridine-1(2H)-carboxylate (**83**)

1H NMR ($CDCl_3$, 400 MHz): 7.50 (d, $J = 8.80$ Hz, 2 H), 7.22 (d, $J = 8.64$ Hz, 2 H), 5.85–5.80 (m, 1 H), 4.65–4.60 (m, 1 H), 5.00–4.93 (m, 1 H), 4.28 (s, 2 H), 4.20–4.07 (m, 1 H), 3.94 (t, $J = 4.95$ Hz, 2 H), 3.65 (t, $J = 4.40$ Hz, 2 H), 3.60–3.63 (m, 1 H), 2.60–3.72 (m, 1 H), 2.34–2.28 (m, 1 H). ^{13}C NMR ($CDCl_3$, 100 MHz): 169.54, 166.82, 156.90, 137.99, 126.12, 123.36, 122.20, 120.36, 81.41, 68.54, 64.11, 61.4, 49.79, 41.50, 28.39, 24.10. MS (ESI) calculated for $C_{22}H_{29}N_3O_5$, $[M + H]^+$, m/z 402.46, found for $[M + Na]^+$, m/z 424.36.

4.15. General procedure for amidation at the ring nitrogen of the core structure to yield **7a**, **7b**, **22–49**, **51**, **58**, **62**, **69–73**, **78**, **79**, **81**, **84**, or **87**

To a stirred solution of organic acid (1.0 mmol) in anhydrous CH_2Cl_2 (5 mL) was added 1-Ethyl-3-(3-dimethylaminopropyl) carbodiimide (EDCI, 1.1 mmol) and DMAP (1.1 mmol) at RT under nitrogen atmosphere. The unprotected form (free amine) of (**6**, **12–21**, **50**, **57**, **61**, **67**, **68**, **76**, **77**, **80**, **83**, or **86**) (1.1 mmol) in anhydrous CH_2Cl_2 (5 mL) was then added drop-wise. After stirring overnight, the reaction mixture was partitioned between 2.0 N HCl solution (20 mL) and CH_2Cl_2 (30 mL). The organic layer was washed further with 2 N HCl (2 × 10 mL) and saturated NaCl solution (20 mL), dried using anhydrous Na_2SO_4 , and concentrated to give a crude, which purified by flash chromatography using gradient of CH_2Cl_2/CH_3OH as eluting phase to give the desired dicarboxamide product in 70–95% yield. The full spectral characterization of these products is provided as [Supplementary Information](#).

4.15.1. (S)-N-Methyl-N-(4-(2-oxopiperidin-1-yl)phenyl)-2-(thiophene-2-carbonyl)-1,2,3,4-tetrahydroisoquinoline-3-carboxamide (**22**)

1H NMR ($CDCl_3$, 400 MHz): 7.51–7.42 (m, 2 H), 7.41 (d, $J = 0.88$ Hz, 1 H), 7.4–7.39 (m, 1 H), 7.37 (d, $J = 20.08$ Hz, 2 H), 7.12–7.09 (m, 2 H), 7.04–7.00 (m, 3 H), 4.97–4.76 (dd, $J = 14.96$ Hz, $J = 69.36$ Hz, 2 H), 4.9–4.82 (m, 1 H), 3.55 (t, $J = 5.44$ Hz, 2 H), 3.21 (s, 3 H), 2.98–2.85 (m, 2 H), 2.50 (t, $J = 6.44$ Hz, 2 H), 1.90–1.84 (m, 4 H). ^{13}C NMR ($CDCl_3$, 100 MHz): 171.32, 170.07, 162.67, 142.93, 141.12, 137.40, 134.54, 133.10, 129.36, 129.01, 128.17, 127.60, 127.36, 126.88, 126.74, 125.48, 53.06, 51.37, 48.92, 38.00, 32.90, 31.24, 23.50, 21.36. MS (ESI) calculated for $C_{27}H_{27}N_3O_3S$, $[M + H]^+$, m/z 474.59, found for $[M + Na]^+$, m/z 496.21.

4.15.2. (R)-2-(2-(4-Chlorophenyl)acetyl)-N-(4-(3-oxomorpholino)phenyl)-1,2,3,4-tetrahydroisoquinoline-3-carboxamide (**47**)

1H NMR ($CDCl_3$, 400 MHz): 7.57–7.30 (m, 2 H), 7.26–7.20 (m, 2 H), 7.19–7.17 (m, 2 H), 7.16–7.00 (m, 4 H), 6.99–6.68 (m, 2 H), 5.14–4.12 (m, 1 H), 4.75–4.50 (m, 2 H), 4.25 (s, 2 H), 3.95 (t, $J = 4.72$ Hz, 2 H), 3.81 (d, $J = 10.40$ Hz, 2 H), 3.66 (t, $J = 5.20$ Hz, 2 H), 3.38–3.29 (m, 1 H), 3.14–2.92 (m, 1 H). ^{13}C NMR ($CDCl_3$, 100 MHz): 172.23, 169.13, 167.34, 136.97, 136.81, 133.53, 133.09, 132.45, 130.72, 130.28, 130.11, 129.54, 129.00, 128.01, 127.46, 126.75, 125.95, 125.39, 124.21, 122.79, 120.63, 68.29, 63.94, 60.56, 52.53, 46.88, 40.45, 28.12. MS (ESI) calculated for $C_{28}H_{26}ClN_3O_4$, $[M + H]^+$, m/z 504.98, found for $[M + Na]^+$, m/z 526.21.

4.15.3. (S)-2-(2-(4-Chlorophenyl)acetamido)-N-methyl-N-(4-(2-oxopiperidin-1-yl)phenyl)-3-phenyl propanamide (**62**)

1H NMR ($CDCl_3$, 400 MHz): 7.30–7.22 (m, 4 H), 7.21–7.19 (m, 3 H), 7.11 (d, $J = 8.36$ Hz, 2 H), 6.93 (d, $J = 7.72$ Hz, 2 H), 6.84 (d, $J = 7.12$ Hz, 2 H), 4.87–4.82 (q, $J = 7.16$ Hz, $J = 15.08$ Hz, 1 H), 3.69 (t, $J = 4.96$ Hz, 2 H), 3.47 (s, 2 H), 3.22 (s, 3 H), 2.90–2.85 (dd,

$J = 7.16$ Hz, $J = 13.32$, 1 H), 2.71–2.66 (dd, $J = 7.00$ Hz, $J = 13.36$ Hz, 1 H), 2.59 (t, $J = 6.40$, 2 H), 2.05–1.95 (m, 4 H). ^{13}C NMR ($CDCl_3$, 100 MHz): 171.30, 170.07, 169.63, 143.01, 140.21, 136.00, 133.15, 130.62, 129.24, 128.95, 128.44, 127.95, 127.25, 126.90, 51.42, 51.19, 42.76, 38.91, 37.60, 32.93, 23.53, 21.40. MS (ESI) calculated for $C_{29}H_{30}ClN_3O_3$, $[M + H]^+$, m/z 505.03, found for $[M + Na]^+$, m/z 526.33.

4.15.4. (1R, 3S, 4R)-2-(2-(4-Chlorophenyl)acetyl)-N-(4-(3-oxomorpholino)phenyl)-2-azabicyclo [2.2.1]heptane-3-carboxamide (**87**)

1H NMR ($CDCl_3$, 400 MHz): 7.52 (d, $J = 8.64$ Hz, 2 H), 7.32 (d, $J = 8.32$ Hz, 2 H), 7.23 (d, $J = 8.36$ Hz, 2 H), 7.22 (d, $J = 8.20$ Hz, 2 H), 4.32 (s, 2 H), 4.26 (s, 2 H), 4.01 (t, $J = 4.96$ Hz, 2 H), 3.76–3.65 (m, 4 H), 3.11–3.95 (m, 1 H), 2.04–1.99 (m, 1 H), 1.89–1.74 (m, 3 H), 1.63–1.45 (m, 3 H). ^{13}C NMR (CD_3OD , 100 MHz): 171.24, 170.63, 169.48, 138.89, 138.48, 135.06, 133.86, 132.02, 129.63, 127.56, 122.03, 69.07, 67.43, 65.09, 60.21, 51.20, 43.46, 41.58, 36.43, 32.14, 28.55. MS (ESI) calculated for $C_{25}H_{26}ClN_3O_4$, $[M + H]^+$, m/z 468.95, found for $[M + Na]^+$, m/z 490.27.

Acknowledgments

This work was supported by grants RC1 HL099420, R01 HL090586 and P01 HL107152 from the National Institutes of Health.

Appendix A. Supplementary material

Supplementary material associated with this article can be found, in the online version, at <http://dx.doi.org/10.1016/j.ejmech.2012.06.032>.

References

- [1] B.L. Henry, U.R. Desai, Anticoagulants: drug discovery and development, in: D. Rotella, D.J. Abraham (Eds.), *Burger's Medicinal Chemistry*, John Wiley and Sons, New York, 2010, pp. 365–408.
- [2] Y.-K. Lee, M.R. Player, Developments in factor Xa inhibitors for the treatment of thromboembolic disorders, *Med. Res. Rev.* 31 (2011) 202–283.
- [3] J.A. Huntington, T.P. Baglin, Targeting thrombin—rational drug design from natural mechanisms, *Trends Pharmacol. Sci.* 24 (2003) 589–595.
- [4] M. Popović, K. Smiljanić, B. Dobutović, T. Syrovets, T. Simmet, E.R. Isenovič, Thrombin and vascular inflammation, *Mol. Cell. Biochem.* 359 (2012) 301–313.
- [5] K.G. Mann, K. Brummel, S. Butenas, What is all that thrombin for, *J. Thromb. Haemostasis* 1 (2003) 1504–1514.
- [6] E.T. Yin, S. Wessler, Investigation of the apparent thrombogenicity of thrombin, *Thromb. Diath. Haemorrh* 20 (1968) 465–468.
- [7] E.T. Yin, S. Wessler, Heparin-accelerated inhibition of activated factor X by its natural inhibitor, *Biochem. Biophys. Acta* 201 (1970) 387–390.
- [8] S. Wessler, E.T. Yin, Theory and practice of minidose heparin in surgical patients, *Circulation* 47 (1973) 671–676.
- [9] J. Ansell, Factor Xa or thrombin: is factor Xa a better target? *J. Thromb. Haemostasis* 5 (Suppl. 1) (2007) 60–64.
- [10] P.A. Merlini, D. Ardissino, K.A. Bauer, L. Oltrona, A. Pezzano, B. Bottasso, R.D. Rosenberg, P.M. Mannucci, Persistent thrombin generation during heparin therapy in patients with acute coronary syndromes, *Arterioscler. Thromb. Vasc. Biol.* 17 (1997) 1325–1330.
- [11] C. Hermans, D. Claeys, Review of the rebound phenomenon in new anticoagulant treatments, *Curr. Med. Res. Opin.* 22 (2006) 471–481.
- [12] R.A. Rezaie, Prothrombin protects factor Xa in the prothrombinase complex from inhibition by the heparin–antithrombin complex, *Blood* 97 (2001) 2308–2313.
- [13] J.I. Weitz, M. Hudoba, D. Massel, J. Maraganore, J. Hirsh, Clot-bound thrombin is protected from inhibition by heparin–antithrombin III independent inhibitors, *J. Clin. Invest.* 86 (1990) 385–391.
- [14] U.R. Desai, New antithrombin-based anticoagulants, *Med. Res. Rev.* 24 (2004) 151–181.
- [15] R.A. Al-Horani, A. Liang, U.R. Desai, Designing nonsaccharide allosteric activators of antithrombin for accelerated inhibition of factor Xa, *J. Med. Chem.* 54 (2011) 6125–6138.
- [16] A. Straub, S. Roehrig, A. Hillisch, Oral, direct thrombin and factor Xa inhibitors: the replacement for warfarin, leeches, and pig intestines? *Angew. Chem. Int. Ed.* 50 (2011) 4574–4590.
- [17] B.L. Henry, B.H. Monien, P.E. Bock, U.R. Desai, A novel allosteric pathway of thrombin inhibition. Exosite II mediated potent inhibition of thrombin by

- chemo-enzymatic, sulfated dehydropolymers of 4-hydroxycinnamic acids, *J. Biol. Chem.* 282 (2007) 31891–31899.
- [18] P.S. Sidhu, A. Liang, A.Y. Mehta, M.H. Abdel Aziz, Q. Zhou, U.R. Desai, Rational design of potent, small, synthetic allosteric inhibitors of thrombin, *J. Med. Chem.* 54 (2011) 5522–5531.
 - [19] Y. Xu, S. Masuko, M. Takiuddin, H. Xu, R. Liu, J. Jing, S.A. Mousa, R.J. Linhardt, J. Liu, Chemoenzymatic synthesis of homogeneous ultralow molecular weight heparins, *Science* 334 (2011) 498–501.
 - [20] G.T. Gunnarsson, U.R. Desai, Designing small, non-sugar activators of antithrombin using hydrophobic interaction analyses, *J. Med. Chem.* 45 (2002) 1233–1243.
 - [21] A. Raghuraman, A. Liang, C. Krishnasamy, T. Lauck, C.T. Gunnarsson, U.R. Desai, On designing non-saccharide, allosteric activators of antithrombin, *Eur. J. Med. Chem.* 44 (2009) 2626–2631.
 - [22] E. Perzborn, S. Roehrig, A. Straub, D. Kubitz, F. Misselwitz, The discovery and development of rivaroxaban, an oral, direct factor Xa inhibitor, *Nat. Rev. Drug Discov.* 10 (2011) 61–75.
 - [23] D.J.P. Pinto, M.J. Orwat, S. Koch, K.A. Rossi, R.S. Alexander, A. Smallwood, P.C. Wong, A.R. Rendina, J.M. Luetting, R.M. Knabb, K. He, B. Xin, R.R. Wexler, P.Y.S. Lam, Discovery of 1-(4-methoxyphenyl)-7-oxo-6-(4-(2-oxopiperidin-1-yl)phenyl)-4,5,6,7-tetrahydro-1H-pyrazolo[3,4-c]pyridine-3-carboxamide (Apixaban, BMS-562247), a highly potent, selective, efficacious, and orally bioavailable inhibitor of blood coagulation factor Xa, *J. Med. Chem.* 50 (2007) 5339–5356.
 - [24] D.J. Pinto, D.M.J. Orwat, S. Wang, J.M. Fevig, M.L. Quan, E. Amparo, J. Cacciola, K.A. Rossi, R.S. Alexander, A.M. Smallwood, J.M. Luetting, L. Liang, B.J. Augst, M.R. Wright, R.M. Knabb, P.C. Wong, R.R. Wexler, P.Y. Lam, Discovery of 1-[3-(aminomethyl)phenyl]-N-[3-fluoro-2'-(methylsulfonyl)-[1,1'-biphenyl]-4-yl]-3-(trifluoromethyl)-1H-pyrazole-5-carboxamide (DPC423), a highly potent, selective, and orally bioavailable inhibitor of blood coagulation factor Xa, *J. Med. Chem.* 44 (2001) 566–578.
 - [25] Y. Imaeda, T. Kuroita, H. Sakamoto, T. Kawamoto, M. Tobisu, N. Konishi, K. Hiroe, M. Kawamura, T. Tanaka, K. Kubo, Discovery of imidazo[1,5-c]imidazol-3-ones: weakly basic, orally active factor Xa inhibitors, *J. Med. Chem.* 51 (2008) 3422–3436.
 - [26] S. Maignan, J.P. Guilloteau, Y.M. Choi-Sledeski, M.R. Becker, W.R. Ewing, H.W. Pauls, A.P. Spada, V. Mikol, Molecular structures of human factor Xa complexed with ketopiperazine inhibitors: preference for a neutral group in the S1 pocket, *J. Med. Chem.* 46 (2003) 685–690.
 - [27] T. Nagata, T. Yoshino, N. Haginoya, K. Yoshikawa, M. Nagamochi, S. Kobayashi, S. Komoriya, A. Yokomizo, R. Muto, M. Yamaguchi, K. Osanai, M. Suzuki, H. Kanno, Discovery of N-[[1,2,5,5S]-2-[(5-chloroindol-2-yl)carbonyl]amino]-5-(dimethylcarbamoyl)cyclohexyl]-5-methyl-4,5,6,7-tetrahydrothiazolo[5,4-c]pyridine-2-carboxamide hydrochloride: a novel, potent and orally active direct inhibitor of factor Xa, *Bioorg. Med. Chem.* 17 (2009) 1193–1206.
 - [28] R.J. Young, A.D. Borthwick, D. Brown, C.L. Burns-Kurtis, M. Campbell, C. Chan, M. Charbaut, C.W. Chung, M.A. Convery, H.A. Kelly, N.P. King, S. Kleantous, A.M. Mason, A.J. Pateman, A.N. Patikis, I.L. Pinto, D.R. Pollard, S. Senger, G.P. Shah, J.R. Toomey, N.S. Watson, H.E. Weston, Structure and property based design of factor Xa inhibitors: pyrrolidin-2-ones with biaryl P4 motifs, *Bioorg. Med. Chem. Lett.* 18 (2008) 23–27.
 - [29] J.M. Smallheer, S. Wang, M.L. Laws, S. Nakajima, Z. Hu, W. Han, I. Jacobson, J.M. Luetting, K.A. Rossi, A.R. Rendina, R.M. Knabb, R.R. Wexler, P.Y.S. Lam, M.L. Quan, Sulfonamidolactam inhibitors of coagulation factor Xa, *Bioorg. Med. Chem. Lett.* 18 (2008) 2428–2433.
 - [30] S. Roehrig, A. Straub, J. Pohlmann, T. Lampe, S. Pernerstorfer, K.H. Schlemmer, P. Reinemer, E. Perzborn, Discovery of the novel antithrombotic agent 5-chloro-N-(((5S)-2-oxo-3-[4-(3-oxomorpholin-4-yl)phenyl]-1,3-oxazolidin-5-yl)methyl)thiophene-2-carboxamide (BAY 59-7939): An oral, direct factor Xa inhibitor, *J. Med. Chem.* 48 (2005) 5900–5908.
 - [31] J.T. Kohrt, K.J. Filipinski, W.L. Cody, C.F. Bigge, F. La, K. Welch, T. Dahring, J.W. Bryant, D. Leonard, G. Bolton, L. Narasimhan, E. Zhang, J.T. Peterson, S. Haarer, V. Sahasrabudhe, N. Janiczek, S. Desiraju, M. Hena, C. Fiakpui, N. Saraswat, R. Sharma, S. Sun, S.N. Maiti, R. Leadley, J.J. Edmunds, The discovery of glycine and related amino acid-based factor Xa inhibitors, *Bioorg. Med. Chem.* 14 (2006) 4379–4392.
 - [32] C.A. Van Huis, A. Casimiro-Garcia, C.F. Bigge, W.L. Cody, D.A. Dudley, K.J. Filipinski, R.J. Heemstra, J.T. Kohrt, R.J. Leadley Jr., L.S. Narasimhan, T. McClanahan, I. Mochalkin, M. Pamment, J. Thomas Peterson, V. Sahasrabudhe, R.P. Schaum, J.J. Edmunds, Exploration of 4,4-disubstituted pyrrolidine-1,2-dicarboxamides as potent, orally active factor Xa inhibitors with extended duration of action, *Bioorg. Med. Chem.* 17 (2009) 2501–2511.
 - [33] B. Ye, D.O. Arnaiz, Y.L. Chou, B.D. Griedel, R. Karanjawala, W. Lee, M.M. Morrissey, K.L. Sacchi, S.T. Sakata, K.J. Shaw, S.C. Wu, Z. Zhao, M. Adler, S. Cheeseman, W.P. Dole, J. Ewing, R. Fitch, D. Lentz, A. Liang, D. Light, J. Morser, J. Post, G. Rumennik, B. Subramanyam, M.E. Sullivan, R. Vergona, J. Walters, Y.X. Wang, K.A. White, M. Whitlow, M.J. Kochanny, Thiophene-anthranilamides as highly potent and orally available factor Xa inhibitors, *J. Med. Chem.* 50 (2007) 2967–2980.
 - [34] J.R. Pruitt, D.J. Pinto, M.J. Estrella, L.L. Bostrom, R.M. Knabb, P.C. Wong, M.R. Wright, R.R. Wexler, Isoxazolines and isoxazoles as factor Xa inhibitors, *Bioorg. Med. Chem. Lett.* 10 (2000) 685–689.
 - [35] M.L. Quan, P.Y.S. Lam, Q. Han, D.J.P. Pinto, M.Y. He, E. Renhua, D. Christopher, C.G. Clark, C.A. Teleha, J.H. Sun, R.S. Alexander, S. Bai, J.M. Luetting, R.M. Knabb, P.C. Wong, R.R. Wexler, Discovery of 1-(3'-aminobenzisoxazol-5'-yl)-3-trifluoromethyl-N-[2-fluoro-4-[(2'-dimethylamino-methyl)imidazol-1-yl]phenyl]-1H-pyrazole-5-carboxamide hydrochloride (Razaxaban), a highly potent, selective, and orally bioavailable factor Xa inhibitor, *J. Med. Chem.* 48 (2005) 1729–1744.
 - [36] Y.K. Lee, D.J. Parks, T. Lu, T.V. Thieu, T. Markotan, W. Pan, D.F. McComsey, K.L. Milkiewicz, C.S. Cryslar, N. Ninan, M.C. Abad, E.C. Giardino, B.E. Maryanoff, B.P. Damiano, M.R. Player, 7-Fluoroindazoles as potent and selective inhibitors of factor Xa, *J. Med. Chem.* 51 (2008) 282–297.
 - [37] H. Matter, E. Defossa, U. Heinelt, P.M. Blohm, D. Schneider, A. Müller, S. Herok, H. Schreuder, A. Liesum, V. Brachvogel, P. Lönze, A. Walser, F. Al-Obeidi, P. Wildgoose, Design and quantitative structure–activity relationship of 3-amidinobenzyl-1H-indole-2-carboxamides as potent, nonchiral, and selective inhibitors of blood coagulation factor Xa, *J. Med. Chem.* 45 (2002) 2749–2769.
 - [38] M. Nazaré, D.W. Will, H. Matter, H. Schreuder, K. Ritter, M. Urmann, M. Essrich, A. Bauer, M. Wagner, J. Czech, M. Lorenz, V. Laux, V. Wehner, Probing the subpockets of factor Xa reveals two binding modes for inhibitors based on a 2-carboxyindole scaffold: a study combining structure–activity relationship and X-ray crystallography, *J. Med. Chem.* 48 (2005) 4511–4525.
 - [39] D.J.P. Pinto, R.A. Gallema Jr., M.L. Quan, M.J. Orwat, C. Clark, R. Li, B. Wells, F. Woerner, R.S. Alexander, K.A. Rossi, A. Smallwood, P.C. Wong, J.M. Luetting, A.R. Rendina, R.M. Knabb, K. He, R.R. Wexler, P.Y.S. Lam, Discovery of potent, efficacious, and orally bioavailable inhibitors of blood coagulation factor Xa with neutral P1 moieties, *Bioorg. Med. Chem. Lett.* 16 (2006) 5584–5589.
 - [40] B.I. Eriksson, D.J. Quinlan, J.I. Weitz, Comparative pharmacodynamics and pharmacokinetics of oral direct thrombin and factor Xa inhibitors in development, *Clin. Pharmacokinet.* 48 (2009) 1–22.
 - [41] Y. Zhang, J. Feng, C. Liu, L. Zhang, J. Jiao, H. Fang, L. Su, X. Zhang, J. Zhang, M. Li, B. Wang, W. Xu, Design, synthesis, and preliminary activity assay of 1,2,3,4-tetrahydro-isquinoline-3-carboxylic acid derivatives as novel histone deacetylases (HDACs) inhibitors, *Bioorg. Med. Chem.* 18 (2010) 1761–1772.
 - [42] S. Cheng, X. Zhang, W. Wang, M. Zhao, M. Zheng, H.W. Chang, J. Wu, S. Peng, A class of novel N-(3S-1,2,3,4-tetrahydroisquinoline-3-carbonyl)-L-amino acid derivatives: their synthesis, antithrombotic activity evaluation, and 3D QSAR analysis, *Eur. J. Med. Chem.* 44 (2009) 4904–4919.
 - [43] S. Azukizawa, M. Kasai, K. Takahashi, T. Miike, K. Kunishiro, M. Kanda, C. Mukai, H. Shirahase, Synthesis and biological evaluation of (S)-1,2,3,4-tetrahydroisquinoline-3-carboxylic acids: a novel series of PPAR γ agonists, *Chem. Pharm. Bull.* 56 (2008) 335–345.
 - [44] T.B. Cai, Z. Zou, J.B. Thomas, L. Brieady, H.A. Navarro, F.I. Carroll, Synthesis and in vitro opioid receptor functional antagonism of analogues of the selective kappa opioid receptor antagonist (3R)-7-hydroxy-N-((1S)-1-(((3R,4R)-4-(3-hydroxyphenyl)-3,4-dimethyl-1-piperidinyl)methyl)-2-methylpropyl)-1,2,3,4-tetrahydro-3-isoquinolinecarboxamide (JDTic), *J. Med. Chem.* 51 (2008) 1849–1860.
 - [45] C.A.G.N. Montalbetti, V. Falque, Amide bond formation and peptide coupling, *Tetrahedron* 61 (2005) 10827–10852.
 - [46] A. Klapars, X. Huang, S.L. Buchwald, A general and efficient copper catalyst for the amidation of aryl halides, *J. Am. Chem. Soc.* 124 (2002) 7421–7428.
 - [47] D.M. Shendage, R. Froehlich, G. Haupe, Highly efficient stereoconservative amidation and deamidation of α -amino acids, *Org. Lett.* 6 (2004) 3675–3678.
 - [48] L.J. Mathias, W.D. Fuller, D. Nissen, M. Goodman, Polydepsipeptides. 6. Synthesis of sequential polymers containing varying ratios of L-alanine and L-lactic acid, *Macromolecules* 11 (1978) 534–539.
 - [49] J. Verghese, A. Liang, P.P. Sidhu, M. Hindle, Q. Zhou, U.R. Desai, First steps in the direction of synthetic, allosteric, direct inhibitors of thrombin and factor Xa, *Bioorg. Med. Chem. Lett.* 19 (2009) 4126–4129.
 - [50] D.J.P. Pinto, J.M. Smallheer, D.L. Cheney, R.M. Knabb, R.R. Wexler, Factor Xa inhibitors: next-generation antithrombotic agents, *J. Med. Chem.* 53 (2010) 6243–6274.
 - [51] R.J. Young, The successful quest for oral factor Xa inhibitors; learnings for all of medicinal chemistry? *Bioorg. Med. Chem. Lett.* 21 (2011) 6228–6235.
 - [52] H.-J. Rupprecht, R. Blank, Clinical pharmacology of direct and indirect factor Xa inhibitors, *Drugs* 70 (2010) 2153–2170.
 - [53] B.L. Henry, J.N. Thakkar, E.J. Martin, D.F. Brophy, U.R. Desai, Characterization of the plasma and blood anticoagulant potential of structurally and mechanistically novel oligomers of 4-hydroxycinnamic acids, *Blood Coagul. Fibrinolysis* 20 (2009) 27–34.
 - [54] B.H. Monien, B.L. Henry, A. Raghuraman, M. Hindle, U.R. Desai, Novel chemo-enzymatic oligomers of cinnamic acids as direct and indirect inhibitors of coagulation proteinases, *Bioorg. Med. Chem.* 14 (2006) 7988–7998.
 - [55] W.A. Schumacher, S.E. Seiler, T.E. Steinbacher, A.B. Stewart, J.S. Bostwick, K.S. Hartl, E.C. Liu, M.L. Ogletree, Antithrombotic and hemostatic effects of a small molecule factor Xla inhibitor in rats, *Eur. J. Pharmacol.* 570 (2007) 167–174.